MODELLING OF RESONANCE RESPONSE OF DAWEI SEAPORT TO TSUNAMI WAVES

Yang Zhang[1] , Onodera Maki[2] and Chris Carr[3]

A numerical model based on the nonlinear shallow water equations was used to investigate the response of the Dawei Seaport to approaching synthetic tsunami waves. Dawei Port is a new mega deep seaport currently under development, located on southeastern coast of Myanmar just north of the city of Dawei. Tsunami waves at the model boundary were determined based on post-tsunami surveys along the Myanmar coastline from the 2004 Indian Ocean Tsunami, and further sensitivity tests on tsunami wave periods were performed. Model results show that the largest amplification of the tsunami wave within the inner port is over 5 times, associated with wave period of 40 minutes. This is in good agreement with the fundamental natural period of 36.5 minutes determined by a white-noise analysis using a local Boussinesq model. Sensitivity tests suggest that tsunami amplification increases with the coincident tide level, and if a tsunami (2m in height and 20 minute in period) similar to the 2004 tsunami were to arrive at high tide, the tsunami elevation would exceed the proposed deck level and likely cause flooding of port facilities. As tsunami waves approach the port area, strong rotational currents are predicted at the port entrance area and in the outer harbor of the port, and topographically-controlled jet-like strong currents are predicted in the primary basin. The strongest currents with flow speeds well over 2m/s and 3m/s for tsunami wave periods of 20 minutes and 40 minutes, respectively, are expected around tips of the breakwaters, at the port entrance and in the primary basin.

Keywords: tsunami; Dawei port; port response; resonance response; amplification; tsunami waves; tsunami currents; rotational currents; natural periods; fundamental modes

Introduction

Large harbors have natural resonance periods ranging from several to tens of minutes, which are comparable to tsunami wave periods. Therefore, tsunamis can be an important mechanism for excitation of large harbors (Barua et al., 2006; Huang and Lee, 2012). Resonant amplification of the tsunami waves can cause overtopping, high mooring loads on vessels and berthing facilities. In addition, very strong currents associated with tsunamis in ports and harbors can break mooring lines and detach large vessels from berthing locations. Extreme tsunami currents can also lead to scour damage of breakwaters and other coastal structures. During the 2004 Indian Ocean Tsunami, damages to ports and harbors were reported in a series of papers by Okal et al. (2006a,b,c). The most remarkable of these events occurred in the port of Salalah, Oman, approximately 4000km away from the earthquake epicenter. About 90 minutes after tsunami first arrival, strong currents near the most offshore uploading berth broke all the mooring lines on a 285-m vessel and pulled it away from the berth. The vessel was then caught in a system of energetic eddies and drifted on the currents for several hours. The vessel reached the far side of the breakwater but did not make contact with the breakwater, subsequently traveled further offshore and eventually grounded on a sand bar on the north side of the harbor. More recently, damages caused by the 2011 Tohoku Tsunami to a number of ports and harbors on both sides of the Pacific have been observed.

Dawei Port is a new mega seaport that is currently under development, and is located at southeastern coast of Myanmar. The Myanmar coast has been affected by a number of tsunamis, including the December 26, 2004 Indian Ocean Tsunami. The 2004 tsunami was generated by the third largest earthquake recorded (surpassed only by the 1960 Chile earthquake and the 1964 Alaska earthquake) with its epicenter located 80km west of the northern Sumatra coast. The 2004 Indian Ocean Tsunami is one of the most devastating natural disasters in the last century, causing more than 292,000 fatalities in 12 countries bordering the Indian Ocean basin. Field surveys show that the largest tsunami runup (up to 30m) occurred south of Banda Aceh, Sumatra, and a tsunami runup of over 10m was also observed along the Thailand coast. Based on post-tsunami site reconnaissance surveys, tsunami heights along the Myanmar coast were generally in the range of 1 to 3m, and are estimated to be in the range of 2m in the project area.

This paper presents the numerical modelling study performed to investigate resonance response of the proposed Dawei Port layout to tsunami waves with various periods. A numerical model based on the shallow water equations has been developed to simulate the propagation of the tsunami waves, and to evaluate the tsunami elevation and tsunami induced currents within the port and along the breakwaters under attack of tsunami waves. A white-noise simulation using a Boussinesq model was also carried out to reveal the natural resonance modes of the port. Sensitivity tests on coincident tide level and bottom friction were conducted to examine the uncertainty of the model results.

[1] CH2M HILL Inc., 1101 Channelside Dr., Tampa, Florida, 33602, US
[2] CH2M HILL Inc., 22 Cortlandt St, 30th floor , New York, New York, 10007, US
[3] Formerly of Halcrow, a CH2M HILL Company, 22 Cortlandt St, 30th floor, New York, New York, 10007, US

Dawei Seaport Development

Dawei Seaport is part of an overall industrial development project initiated by the Myanmar government and comprises an industrial estate, new township, steel mill, power plants, and a transborder highway connecting Dawei to the Thai border. In November 2010 the Italian-Thai Development Public Company Limited (ITD) was awarded a concession to implement this ambitious project with the support of the government of Myanmar and Thailand. The Dawei Port is located in the northern part of the Maungmagan Bay, approximately 28 km north of the provincial city of Dawei in Myanmar. The Dawei Deep Seaport will serve as a new commercial gateway providing an alternative sea route that bypasses the crowded Malacca Straits to India, the Middle East, Africa, and Europe. With the road and rail links that will be developed between China, Thailand, and Myanmar, Dawei is strategically located to become a regional logistics and trading hub. Dawei is also an integral part of the Greater Mekong Sub-region South Corridor, which will connect Dawei in the west via Bangkok in the center and Ho Chi Minh City and Quy Nhon in Vietnam to the east.

The port is comprised of an outer harbor which is delineated by the Main breakwater and the Lee breakwater, the inner harbor, and a deep-draft approach channel, see Figure 1. The approach channel is approximately10 km long, 20 m deep, and 350m wide. The Main Breakwater (approximately 3 km long) and the Lee Breakwater (approximately 1.5 km long) will be constructed as dynamically stable berm breakwaters. The outer harbor accommodates the steel mill berths, the liquid bulk berths, LNG berths, and a tug harbor, and will be dredged to -16m. The inner harbor comprises a primary basin and secondary basin, and accommodates container, general cargo and fertilizer terminals over nearly 10km of quay walls. The primary and secondary basins are planned to have a dredge depth of -16.5mCD, and will be 500m and 350m wide, respectively. The port also includes revetments, access roads, stormwater drainage, and port utilities. The Dawei Sea Port will be developed in multiple phases over a period of 25 years and when fully developed by 2040, the port will include 8 container berths, 28 general cargo berths, 2 thermal coal berths, 2 fertilizer berths, 5 dry bulk berths for iron ore, coal, and coke, 9 liquid bulk berths, 2 LNG berths, and a tug boat base.

It is worth pointing out that the tsunami modelling investigation was carried out for an earlier version of the port layout, and the port layout was subsequently adjusted to a minor extent based on other considerations. However, as the difference in layout was only marginal, it can be expected that the impact of the change in the port layout on the tsunami response should be minimal and thus the tsunami modelling was not repeated for the revised port layout.

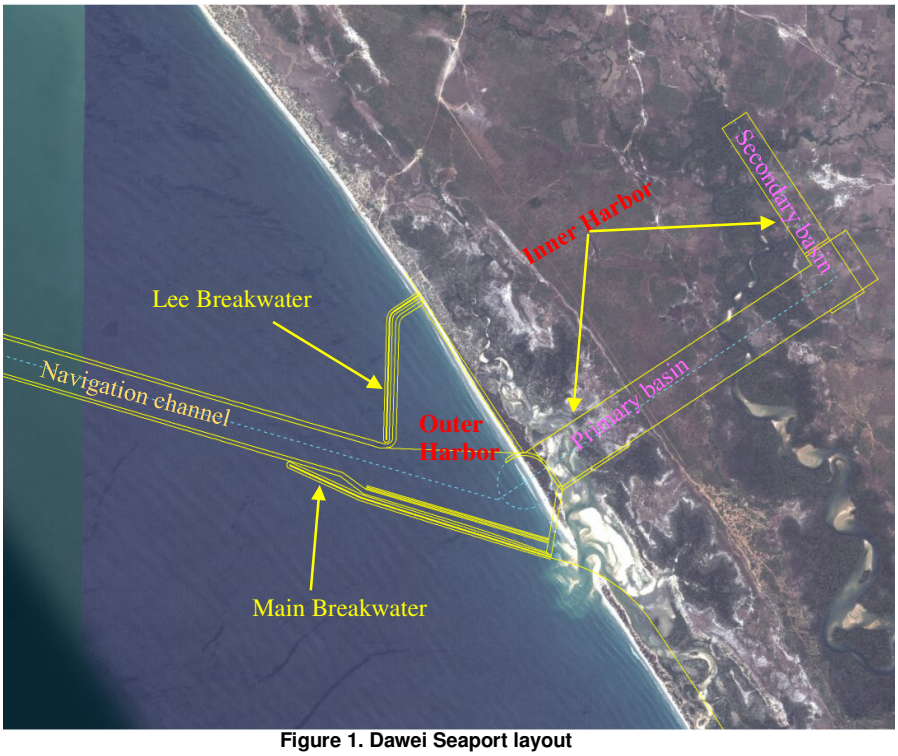

Figure 1. Dawei Seaport layout

Numerical Model

A numerical model, based on DHI's MIKE21 FM HD model solving the nonlinear shallow water equations (NSWE), was developed to simulate the tsunami propagation from offshore to inshore and to assess the resonance response of the port. The NSWE governing equations can be written as:

$$\begin{aligned} &\frac{\partial H}{\partial t}+\frac{\partial (Hu)}{\partial x}+\frac{\partial (Hv)}{\partial y}=0 \\ &\frac{\partial (Hu)}{\partial t}+\frac{\partial (Huu)}{\partial x}+\frac{\partial (Huv)}{\partial y}=fvH-gH\frac{\partial \eta}{\partial x}+\tau_x+\tau'_x \\ &\frac{\partial (Hv)}{\partial t}+\frac{\partial (Huv)}{\partial x}+\frac{\partial (Hvv)}{\partial y}=-fuH-gH\frac{\partial \eta}{\partial y}+\tau_y+\tau'_y \end{aligned} \tag{1}$$

where, $H=\eta+h$ is the total water depth, η the surface elevation, h water depth. (u,v) are depth-averaged velocities in (x,y) directions; g is the gravity acceleration; $f$denotes the Coriolis force coefficient; (τ_x,τ_y) represent the bottom friction effect; (τ'_x,τ'_y) denote eddy viscosity terms.

The nonlinear shallow water equations do not include frequency dispersion effects on wave propagation, and past studies have demonstrated that the dispersive effects could be significant over long propagation distance in deep water (e.g., Grilli et al. 2007; Kirby et al. 2013; among others). On the other hand, Ioualalen et al. (2007) and Grilli et al. (2007) also showed the dispersive effects are negligible on the east side of generation source of the 2004 Indian Ocean Tsunami due to the short propagation distance and also the relatively shallow water depths. Thus, it is appropriate to employ NSWE in this study to investigate the resonance response of the port to approaching tsunami waves. The NSWE have been used in the literature (e.g. Wang and Liu, 2006; Barua et al., 2006; among others) to simulate tsunami propagation.

Post-tsunami reconnaissance surveys along the Myanmar costal area from the Indian Ocean Tsunami were conducted by a team of Myanmar and Japanese scientists in March 2005 (Satake et al. 2006). At Maungmagan beach (Dawei Port is located at the northern portion of the bay), two parallel lines of debris were observed. An interview with a local fisherman suggested that the lower debris line was formed by the tsunami. The interviewee observed that the tsunami arrived at around 2 pm, in a total of four successive waves with 3 to 4 m height. The tsunami arrived at low tide and did not exceed the high tide level of the rainy season, which is the higher debris line. Measurements indicated that the lower and higher debris lines were 2.4 m and 2.9 m above the sea level at the time of measurement. The dune, to which the tsunami did not reach, was 4.0 m high. By subtracting the tide level at the time of tsunami arrival, the tsunami height was suggested to be around 1.8 m. Interviews with local villagers and eyewitnesses at other locations along the shoreline in the Dawei area suggested that the tsunami arrived in three successive waves with interval periods in the range of 5 to 20 minutes.

Model Domain and Model Bathymetry

The main purposes of this study is to investigate the resonance response of the Dawei Port to possible tsunami waves and to assess the water level and flow conditions along the breakwaters and inside the port. Simulation of tsunami generation due to earthquake is beyond the scope of this study. A relatively small model domain (see Figure 2), covering an area of approximately 220km in the alongshore direction by 65km in the cross-shore direction, was used to simulate propagation of the approaching tsunami to the project area.

The model bathymetry was developed based on 3 bathymetry data sources used in the decreasing order of priority: 1) the high-definition bathymetric and topographic data for the project area from a survey conducted in 2008, 2) bathymetry data from DHI C-MAP data base for the reminder nearshore area not covered by the survey, and 3) the ETOPO2 bathymetry data for the offshore area. The model employs an unstructured flexible mesh, and the computational mesh is increasingly refined towards the project area, with the nominal grid sizes decreasing from 2km at offshore to approximately 100m in the port area. The model computational mesh and the resulting model bathymetry contours are shown in Figure 3.

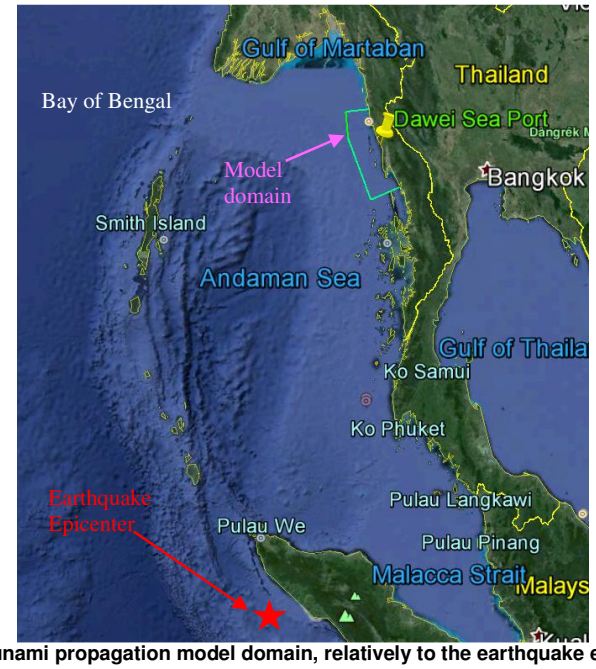

Figure 2. Tsunami propagation model domain, relatively to the earthquake epicenter.

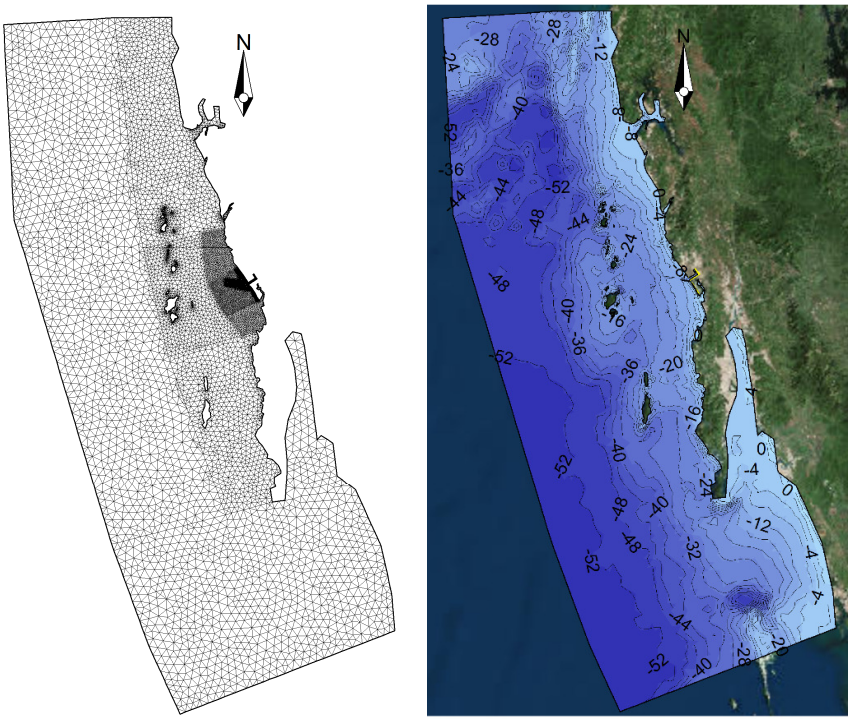

Figure 3. Model computational mesh (left) and bathymetry (right).

Boundary Conditions

Sinusoidal waves were assumed to represent the incident tsunami at the offshore open boundary of the numerical model. Based on post-tsunami reconnaissance surveys for Myanmar from the 2004 Indian Ocean Tsunami, tsunami heights were slightly less than 2m at the survey locations around the Dawei area, with periods in the range of 5 to 20 minutes. Hence, tsunami waves with 2m in height and a period of 20 minutes were adopted as the base case for the modelling. Sensitivity tests on various tsunami wave periods, from 10 to 120 minutes, were subsequently carried out to investigate the resonance response of the port to different tsunami periods. As most interviewees suggested that 3 successive waves were

observed along the coastline in the project area, a series of 3 waves, with an initial depression wave trough, were used in the model simulations. The initial simulations were carried out at tide-less mean sea level, and a set of sensitivity tests were subsequently carried out to investigate the effect of the tide level on the tsunami response of the port. In addition, sensitivity tests on the bottom friction were also conducted.

Simulation Results

Figure 5 presents the modelled time-series of tsunami surface elevations and tsunami induced currents extracted at different locations for the base case (i.e., tsunami waves 2m in height and 20 minutes in period). Figure 4 shows locations of the 4 extraction points: P1 at -18m depth contour located outside of the port, P2 at the outer harbor, P3 in the primary basin and the most inner point P4 in the secondary basin. It is observed that the amplification of tsunami waves in the outer harbor appears to be insignificant, while increases rapidly toward the inner portion of the port. At the most inner location P4, the maximum trough-to-peak height is largest and predicted to be around 6.4m. Model results show that the current speed in the outer harbor is considerably higher than that outside of the port, and is largest at P3 in the primary basin. This is due to the effect of flow contraction as the width of the flow area is much reduced from the outer harbor to the primary basin.

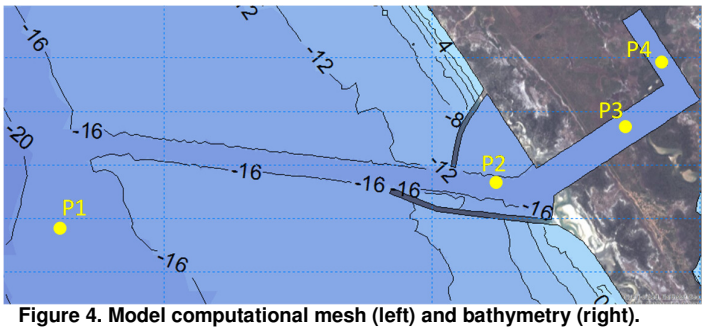

Figure 4. Model computational mesh (left) and bathymetry (right).

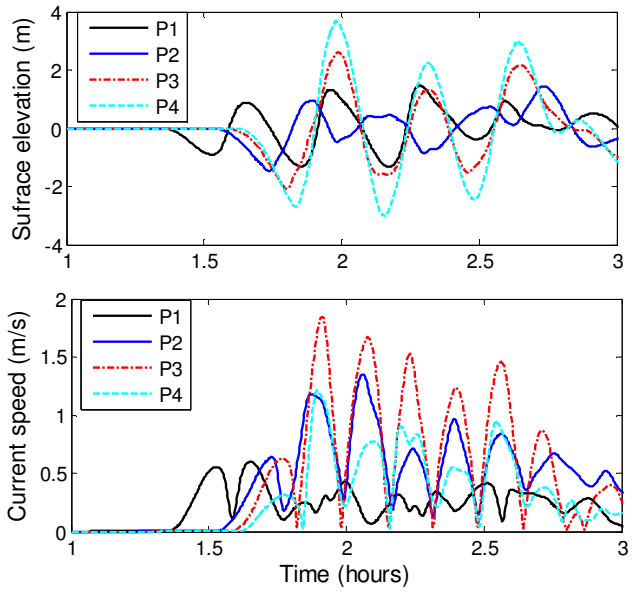

Figure 5. Modelled time-series of tsunami surface elevations (upper) and tsunami induced current speed (lower) at the extraction locations (see Figure 4) for incident tsunami waves with 2m in height and 20 minutes in period

Figure 6 provides snapshots of the modelled typical peak flood flow (water entering the port) and peak ebb flow (water draining out of the port) for the base case (tsunami waves of 2m and 20 minutes) for the port and immediately adjacent nearshore area. As shown, the strong jet-like currents constrained by the quay walls on both sides, are predicted in the primary basin for both the flood flow and ebb flow. Very strong currents, with speeds over 2m/s, are also observed around the tip of the Lee Breakwater and

also along the seaside of the Lee Breakwater. It is interesting to note that the flow directions are opposite between inside and outside of the port (e.g., during the flood flow, the current direction outside the port is towards offshore), suggesting there is a phase lag between the inside and outside of the port. A circulation cell rotating anti-clockwise located right behind the Lee Breakwater during the flood flow is predicted.

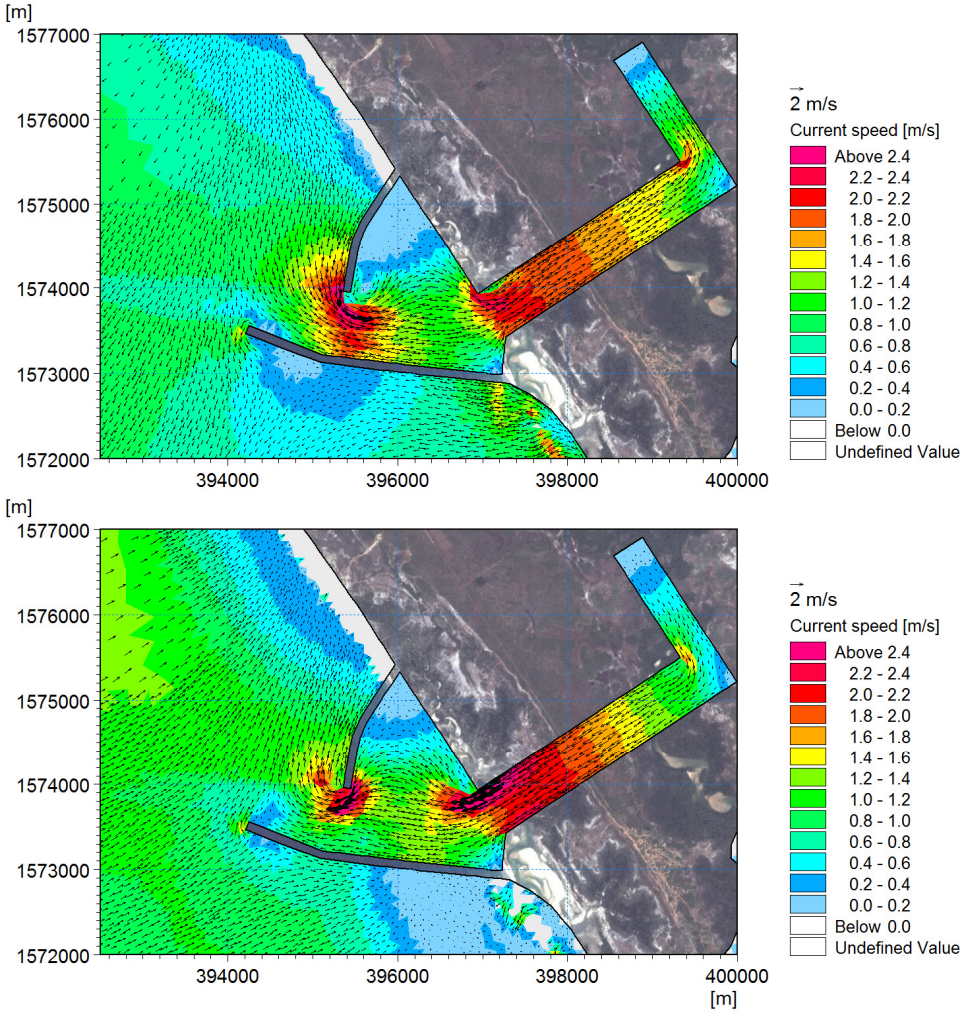

Figure 6. Modelled peak flood flow (upper) and peak ebb flow (lower) for the incident tsunami waves with 2m in height and 20 minutes in period

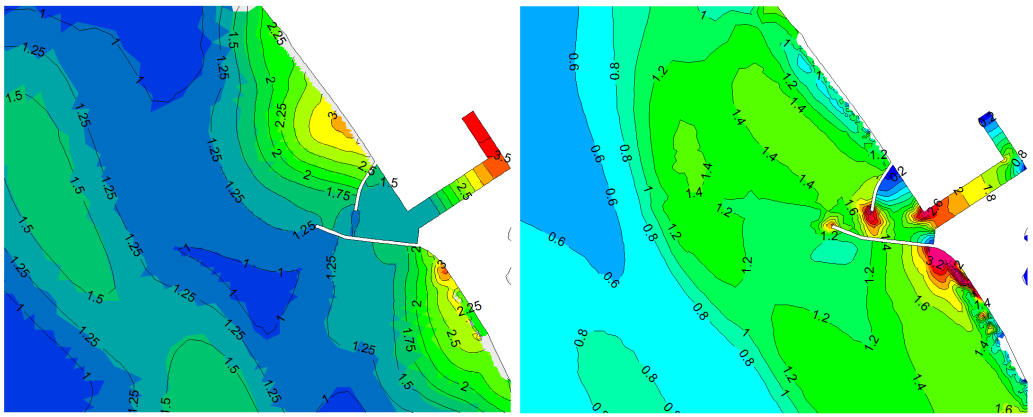

Figure 7. Modelled maximum surface elevation in meter above mean sea level (left) and maximum flow speed in m/s (right) for the incident tsunami waves with 2m in height and 20 minutes in period

Figure 7 shows the maximum tsunami elevation and maximum flow speed in the simulation period for the base case for the port and nearshore area. The tsunami elevation is relative to mean sea level, and it is apparent that the tsunami elevation increases monotonically towards the inner portion of the port. As illustrated, the entrance area to the outer harbor, around the tip of the breakwaters and the primary basin are subject to the strongest currents.

Resonance Response and Amplification Factor

Sensitivity tests have been conducted for a number of wave periods, ranging from 10 minutes to 2 hours to investigate modes of oscillations and resonance period of the port. Amplification of tsunami waves in the port at the most inner location P4 was examined based on simulation results. Amplification factor, which is the ratio of the tsunami wave height in the port to the incident tsunami height at the model boundary (2m), was calculated for each simulation. As aforementioned that since a series of three individual waves was applied at the model boundary for each simulation, the amplification factor was calculated based on the largest wave (i.e., maximum trough-to-crest height). In addition, the maximum tsunami elevation at P4 was also calculated. These results are summarized in Table 1.

Table 1. Amplification factor of tsunami wave height at inner port (P4) varying with wave periods

Run case	Tsunami Period (minutes)	Amplification Factor	Largest Wave	Maximum Tsunami Elevation (m)
1	10	0.90	1st	0.8
2	15	2.42	3rd	2.6
3	20	3.20	1st	3.7
4	30	4.55	2nd	5.6
5	40	5.35	3rd	6.5
6	50	4.82	2nd	6.4
7	60	4.25	1st	5.0
8	90	3.13	1st	3.4
9	120	2.96	1st	3.1

Figure 8 presents the amplification factors at inner port location P4 as a function of tsunami wave periods. As shown, the amplification factor first increases with wave periods and reaches a maximum at 40 minutes, and then decreases with increasing wave periods. The response curve suggests that the resonance period of the port is around 40 minutes. And for this case, the amplification factor is predicted to be 5.35, which is significantly higher than that for the base case, and the maximum tsunami elevation is estimated to be 6.5m above mean sea level.

Snapshots of the modelled peak flood flow and peak ebb flow for wave period of 40 minutes are presented in Figure 9. Large anti-clockwise rotating eddy in the outer harbor is predicted, and similar to the base case, strong currents occur in the port entrance area and topographically-induced jet-like flow is predicted in the primary basin, but generally with enhanced flow speeds. Rotational currents have been observed in a number of ports and harbors during the 2011 Tohoku Tsunami, including Port of Oarai in Japan, and Pillar Point Harbor and Crescent City Harbor in USA (Lynett et al. 2012). An aerial video taken from a helicopter show clear eddy in the Port of Oarai persisting for tens of minutes before it was flushed out by following wave series. Extreme currents with speed up to 4m/s and 5m/s in the Crescent City harbor and Pillar Point harbor respectively, were estimated by local witnesses. Figure 10 shows the maximum tsunami elevation and maximum current speed for this case. The maximum tsunami elevation can be as high as 7m at the inner end of the secondary basin, and the maximum current speeds are highest at the harbor entrance, up to 5m/s. Lynett et al. (2012) used an eddy-resolving model and simulate the sheared and rotational flows observed at the Port of Salalah, Oman during the 2004 Indian Ocean Tsunami. The model predicted a flow speed of approximately 6m/s near the initial location of the vessel pulled away from its moorings as discussed previously, and very strong rotational currents in the port entrance area.

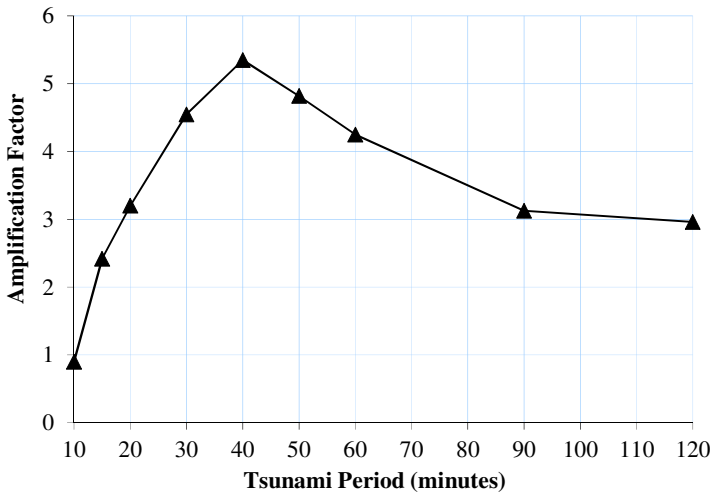

Figure 8. Simulated amplification factor of tsunami wave height at inner port (P4) as a function of tsunami wave periods

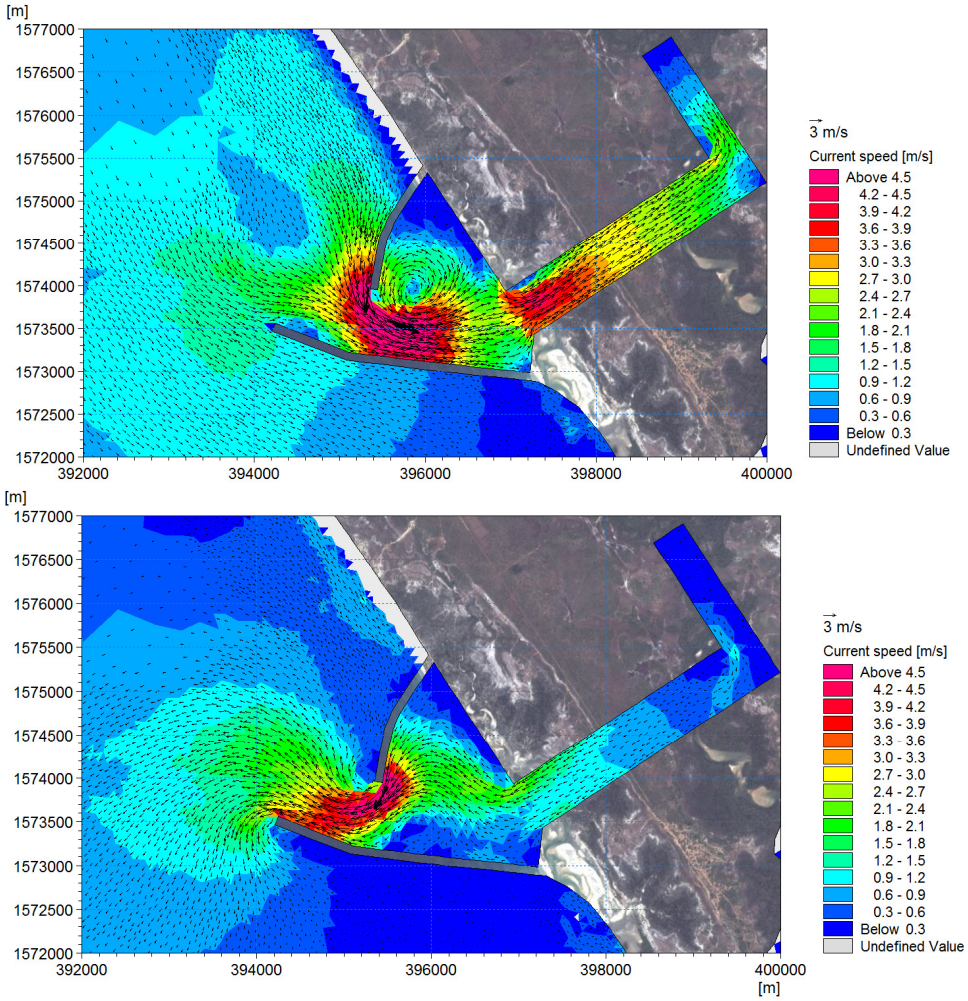

Figure 9. Modelled peak flood flow (upper) and peak ebb flow (lower) for the incident tsunami waves with 2m in height and 40 minutes in period

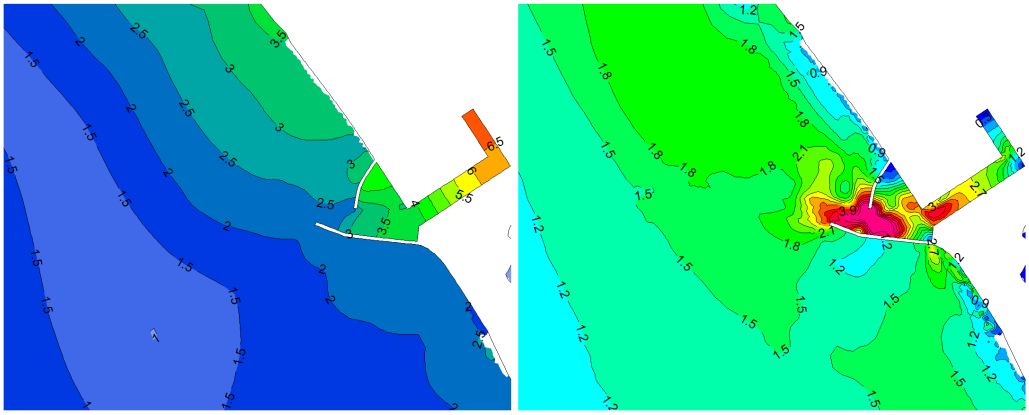

Figure 10. Modelled maximum surface elevation in meter above mean sea level (left) and maximum flow speed in m/s (right) for the incident tsunami waves with 2m in height and 40 minutes in period

Natural Frequencies of the Dawei Port

As an attempt to investigate the natural frequencies of the Dawei Port, a white-noise simulation was conducted using a Boussinesq model covering the local area including the entire port, approach channel and the nearshore area. The simulation was carried out using the incident-wave time-series from a white-noise spectrum. Although not representing a realistic sea state, a simulation with a white-noise spectrum is efficient in revealing the natural resonance modes of any layouts (Gierlevsen et al. 2001). The white-noise spectrum applied represents wave periods from 10s to 6500s, with a small H_{m0}=0.01m. Use of the very small significant wave height is to avoid any nonlinear effects, as the purpose of this experiment was to examine the linear processes.

Spectral analysis of the simulated time-series of surface elevation at extraction point P4 was conducted, and the calculated wave spectrum is shown in Figure 11. As shown, the clear spectral density peaks at frequencies corresponding to periods of 36.5 minutes, 15 minutes, 7.8 minutes and 4.4 minutes, were observed. Among the spectral peaks, the spectral density of the first peak is significantly larger than that of the other 3 peaks, which suggests that the fundamental natural period of the Dawei Port is around 36.5 minutes.

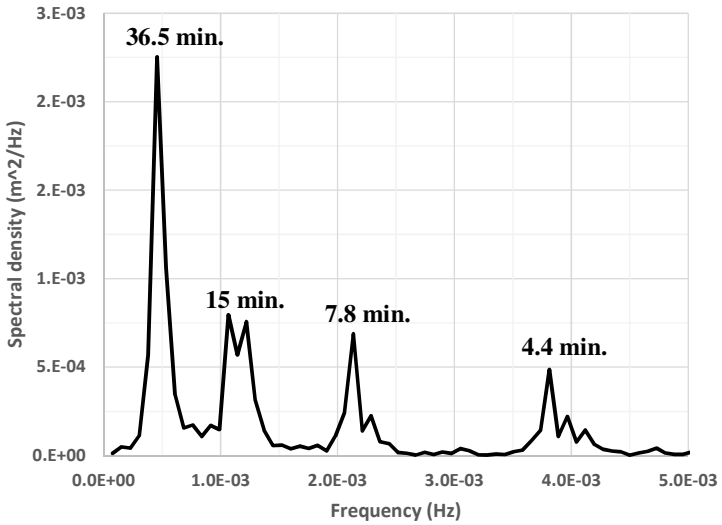

Figure 11. Spectral density of surface elevation time-series at inner port P4 based on the white-noise simulation

The white-noise analysis reveals the natural resonance modes of the port, and the identified fundamental mode (36.5 minutes) agrees well with the investigation on the port response to various tsunami wave periods, which suggests that the largest resonance response of the port is associated with wave period of 40 minutes. It is also interesting to note that as shown in Table 1 for wave periods 15

minutes and 40 minutes, the 3rd individual wave yields the largest wave height, which might be as a result of the resonance response of the port geometry.

Effects of the Tide Level on Tsunami Resonance Response

Tides in the project area can be characterized as semi-diurnal tide with relatively large tidal range. The mean spring tidal range is approximately 4.5m, and peak tidal currents are in the order of 0.3m/s in the nearshore area while minimal inside the port. As typical tsunami wave periods are much shorter than the astronomical tides, tidal level variations are very often neglected in tsunami modelling. However, Kowalik and Proshutinsky (2006), among others, suggested that nonlinear tsunami-tide interactions can be significant, especially when the tidal range is large. In addition, the static change of water depth by a few meters can have an impact on propagation speed and amplification response of the tsunami waves, in particular over shallow water region. To that end, simulations with a high tide level at mean high water spring (MHWS) and a low tide level at mean low water spring (MLWS) were also conducted, and the results were then compared with the base case, in which mean sea level is used.

Comparisons of the amplification factors at inner port location P4 between the 3 different coincident tide levels suggest that amplification of tsunami waves increases with the coincident tide level, as shown in Table 2 and Figure 12. Compared to the base case, amplification factor associated with the high tide is higher by about 10%, and for the low tide level it is approximately 15% less. It is also seen that the maximum tsunami elevation differs significantly between different coincident tide levels, due to the combined effects: 1) relatively large tidal range in this area, and 2) increased amplification of the tsunami waves when coinciding with hide tide. As mentioned previously, the 2004 tsunami arrived at a low tide along the Dawei coastline. The potential flooding and damages could be significantly worse if a similar event occurs during high tide. The model predicts the maximum tsunami elevation at inner port location P4 to be as high as 9.4m above the Lowest Astronomical Tide (LAT), a 3m increase compared to that of the tsunami waves coinciding with mean sea level.

Table 2. Amplification Factor of tsunami wave height at inner port (P4) varying with coincident tide levels

Tide level	Water level (mMSL)	Amplification Factor	Maximum tsunami elevation (mLAT)
MLWS	-2.25	2.7	3.2
MSL	0	3.2	6.4
MHWS	2.25	3.5	9.4

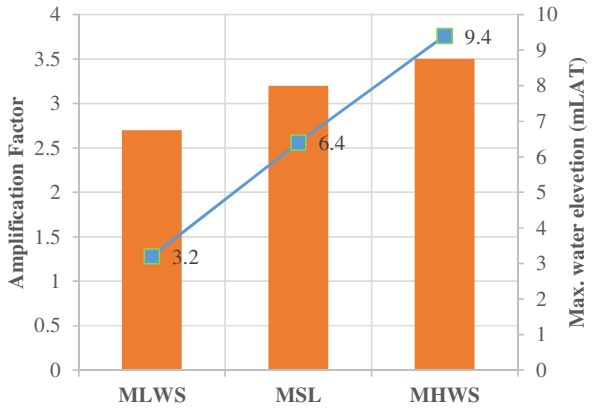

Figure 12. Sensitivity to coincident tide level

Sensitivity Test on Bottom Friction

Effects of bottom friction on tsunami propagation could be important in shallow water, and is a consideration for the onshore portion of the Andaman Sea where the water depth is largely less than 50m. Bottom friction in the model is parameterized using Manning's M number, and its relation to Nikuradse roughness length Ks can be written as $M = 25.4/(Ks\text{^}(1/6))$. To investigate model sensitivity to variation of bottom roughness, several Manning's M values were tested with 2m, 20minutes incident tsunami waves. It should be noted that the larger M values mean less bottom friction. The simulated amplification factors at inner port location P4 versus bottom roughness are shown in Figure 13. The

range of M normally used is from 20 to 40. As indicated, amplification factor decreases by about 20%, when increasing bottom friction from M=40 to M=20.

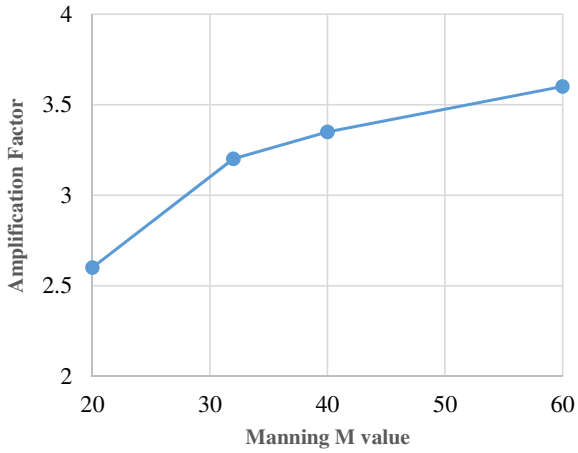

Figure 13. Amplification factors at inner port P4 varying with Manning M value

Discussions and Conclusions

Dawei Seaport is a new mega deep seaport in Myanmar, currently under development. The port will form an important link in global logistics network, providing an alternative route that bypasses the crowded Malacca Straits to India, the Middle East, Africa, and Europe. The port is located in an area that has been affected by a number of tsunamis in the past, including the 2004 Indian Ocean Tsunami. It is therefore important to gain an understanding of the port response to potential tsunami waves. A numerical model based on the nonlinear shallow water equations (NSWE) was established to investigate the port resonance response to incoming tsunami waves. A number of simplifications and assumptions have been used in this study and include the following: First, generation of tsunami waves due to sea floor deformation is beyond the scope of this study. Synthetic tsunami waves, determined based on the post-tsunami surveys from the 2004 tsunami, have been used and propagated to the site. Furthermore, dispersive effects are not included by using the NSWE, which however are expected to be significant only for long distance propagation of tsunami waves over deep water. In addition, tsunami inundation and inland propagation of the tsunami waves are not considered in the model, and this simplification may have some impact on the model results, especially in the secondary basin where overtopping and flooding is most likely to occur.

We simulated tsunami waves with various wave periods from 10 to 120 minutes. Model results show that the largest amplification of tsunami waves in the port results from wave period of 40 minutes. This is in good agreement with the revealed fundamental natural period of approximately 36.5 minutes, which was determined by conducting a white-noise analysis using a small-scale Boussinesq model. Amplification of tsunami waves increases towards the interior part of the port. Inside the secondary basin, amplification factor is over 5 times for the 40 minutes wave period, and is about 3.2 times for the 20 minutes wave period. Model results also suggest that amplification of the tsunami increases with the coincident tide level. For an extreme tsunami event similar to the 2004 Indian Ocean Tsunami (i.e., 2m height and 20-minute period) occurring at a high tide, the peak water level within the port will exceed the proposed deck elevation of +6.7mLAT (which was determined based on the combined total water level of various components, including tides, long term sea level rise, seasonal water level variations and storm surge), resulting in temporary flooding of the site. This, however, was considered as an acceptable risk considering the extremely low occurrence probability for such an event and the high cost associated with implementing mitigation measures.

Very strong tsunami currents are predicted inside the port, with current speeds well over 2m/s and 3m/s for tsunami wave periods of 20 minutes and 40 minutes, respectively. Strong rotational currents are expected at the port entrance and in the outer harbor. In the primary basin, strong jet-like currents constrained by the rectangular shape of the basins are predicted. Without proper precautions in place, these tsunami currents may cause severe damage such as breaking of mooring lines and the free drifting of vessels by the strong currents, resulting in potential vessel-vessel and vessel-port structure collisions. The strong currents could also cause scour and undermining of the breakwaters. The impacts of tsunamis

on ports and harbors should be considered and appropriate mitigation measures should be adopted to minimize disruptions to port operations.

ACKNOWLEDGMENTS

The authors wish to acknowledge Italian-Thai Development Public Company Limited for their financial support and also for allowing us to publish the study.

REFERENCES

Barua D.K., N.F. Allyn, and M.C. Quick. 2006. Modeling Tsunami and Resonance Response of Alberni Inlet, British Columbia, *Proceedings 30th International Conference on Coastal Engineering*, San Deigo, California.

Gierlevsen, T., H. Hebsgaard, and J. Kirkegaard. 2001. Wave Disturbance Modelling in the Port of Sines, Portugal - with special emphasis on the long period oscillations. Singapore, *International Conference on Port and Maritime R&D and Technology*.

Grilli, S.T., M. Ioualalen, J. Asavanant, F. Shi, J.T. Kirby, and P. Watts. 2007. Source constraints and model simulation of the December 26, 2004 Indian Ocean tsunami. *J. Waterway, Port, Coastal Ocean Eng.* 133, 414–428.

Huang, Z. and J.-J. Lee. 2012. Frequency-based harbor response to incident tsunami waves in American Samoa, *Proceedings of 33th International Conference on Coastal Engineering*, ASCE.

Ioualalen, M., J. Asavanant, N. Kaewbanjak, S.T. Grilli, J.T. Kirby, and P. Watts. 2007. Modeling the 26th December 2004 Indian Ocean tsunami: case study of impact in Thailand. *Journal of Geophysical Research,* 112, C07024.

Kenji Satake, Than Tin Aung, Yuki Sawai, Yukinobu Okamura, Kyaw Soe Win, Win Swe, Chit Swe, Tint Lwin Swe, Soe Thura Tun, Maung Maung Soe, Thant Zin Oo, and Saw Htwe Zaw. 2006. Tsunami heights and damage along the Myanmar coast from the December 2004 Sumatra-Andaman earthquake, *Earth Planets Space*, 58, 243-252, 2006

Kirby, J.T., F. Shi, B. Tehranirad, J.C. Harris, and S.T. Grill. 2013. Dispersive tsunami waves in the ocean: Model equations and sensitivity to dispersion and Coriolis effects. *Ocean Modelling*, 66, 39-55.

Kowalik, Z. and Proshutinsky, T. 2006. Tide-Tsunami Interactions, *Science of Tsunami Hazards*, Vol. 24, No. 4, p. 242.

Lynett, P.J., J.C. Borrero, R. Weiss, S. Son, D. Greer and W. Renteria. 2012. Observations and modeling of tsunami-induced currents in ports and harbors, *Earth and Planetary Science Letters*, 327-328, 68-74

Okal, E.A., H.M. Fritz, R. Raveloson, G. Joelson, P. Pancoskova, and G. Rambolamanana. 2006a. Madagascar field survey after the December 2004 Indian Ocean tsunami. *Earthquake Spectra,* 22, S263–S283.

Okal, E.A., H.M. Fritz, P.E. Raad, C.E. Synolakis, Y. Al-Shijbi, and M. Al-Saifi. 2006b. Oman field survey after the December 2004 Indian Ocean tsunami. *Earthquake Spectra,* 22, S203–S218.

Okal, E.A., A. Sladen, H.M. Fritz. 2006c. Mauritius and Réunion Islands, field survey after the December 2004 Indian Ocean tsunami. *Earthquake Spectra*, 22, S241–S261.

Wang, X., Liu, P.L.-F., 2006. An analysis of 2004 Sumatra earthquake fault plane mechanisms and Indian Ocean Tsunami. *J. of Hydraulic Res.* Vol. 00, No. 0, pp. 1-8.